Ecological Indicators 155 (2023) 110928

Contents lists available at ScienceDirect

Ecological Indicators

journal homepage: www.elsevier.com/locate/ecolind

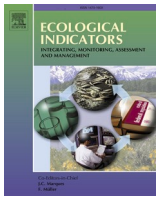

Supply and demand mismatch analysis to improve regulating ecosystem services in Mediterranean urban areas: Insights from four Italian Municipalities

Lina Fusaro [a], Lorenza Nardella [b,*], Fausto Manes [c,*], Alessandro Sebastiani [d], Silvano Fares [a,e]

[a] National Research Council of Italy, Institute of BioEconomy, via dei Taurini 19, Rome 00185, Italy
[b] International PhD Programme/UNESCO Chair "Environment, Resources and Sustainable Development", Department of Science and Technology, Parthenope University of Naples, Via F. Petrarca 80, Naples 80123, Italy
[c] Department of Environmental Biology, Sapienza University of Rome, p.le Aldo Moro 5, Rome 00185, Italy
[d] National Research Council of Italy, Institute on Terrestrial Ecosystems, Strada Provinciale 35d, 9 – 00010, Montelibretti, Italy
[e] National Research Council of Italy, Institute for Agriculture and Forestry Systems in the Mediterranean, P.le Enrico Fermi 1 – Loc. Porto del Granatello, Portici, Naples 80055, Italy

ARTICLE INFO

Keywords:
Air quality
Mismatch analysis
Supply-demand
Mediterranean cities
Urban and *peri*-urban forests

ABSTRACT

Cities are nowadays facing compelling environmental and climatic challenges that threaten human health and well-being; for this reason, enhancing their sustainability and resilience has rapidly ascended to the top of the global and regional political Agenda. The Urban Green Infrastructure represents a key factor in enhancing the environmental quality of cities, and its planning should be steered by a scientifically-sound operationalisation of the Ecosystem Services concept. In this work, we assess the Ecosystem Services mismatch for air quality regulation in four Italian Municipalities (Milan, Bologna, Rome, and Bari), considering the O_3 and PM_{10} pollution; the study frames a geographical gradient (North-South) and has been conducted on a seasonal basis. We propose a composite-indicatorbased approach for estimating the supply and demand of said Ecosystem Services, including the dimensions of air quality and human health, using both geospatial and tabular data. The spatial and temporal features of mismatch allow distinguishing concerns depending on vegetation quantity (green space areas) and quality (functional diversity), structure of urban settlements and cross-cutting criticalities among cities, and to highlight common indicators of mismatch and priority areas for upcoming interventions.

We found that northern cities (Milan and Bologna) suffer a high mismatch, as a result of poor air quality and limited vegetation abundance and functional diversity; southern cities experienced lower demand related to air quality; however, the high mismatch is driven by urban settlement structure and population vulnerability. We also found that compact urbanisation, namely dense urban fabric and the increasing buildings' height, is linked to a marked mismatch regardless of the city's dimension and geographical location.

We believe such an effort is a fundamental step for translating the Ecosystem Services conceptual framework into the development plans of cities, and thus into concrete actions.

Plus, as far as we know, this is one of the first studies explicitly linking urban structure indicators (e.g. building heights and compactness of the urban settlements) to the Ecosystem Services' mismatch.

Abbreviations: ACE, Census Areas; BH, buildings' height; CESDM, Comprehensive Ecosystem Supply-Demand Mismatch; CI, Composite Indices; CLMS, Copernicus Land Monitoring Service; DCC, distance from the city centre; DGA, distance from the closest green area; DI, Demand Index; DU, percentage of high-density urban fabric; ESDM, Ecological Supply-Demand Mismatch; ESs, Ecosystem Services; GCP, Green Cover Percentage; In, average income; LAI, Leaf Area index; LULC, Land Use Land Cover; MDU, percentage of medium-density urban fabric; NBSs, Nature-Based Solutions; PCA, Principal Component Analysis; S2MSI2A, Sentinel 2 MultiSpectral Instrument (Level) 2A; SCP, Semi-automatic Classification Plug-in; SI, Supply Index; UGI, Urban Green Infrastructure; UPUF, percentage of Urban and Peri-Urban forests; Vp, Vegetation potential.

* Corresponding authors.
E-mail addresses: lorenza.nardella001@studenti.uniparthenope.it (L. Nardella), fausto.manes@uniroma1.it (F. Manes).

https://doi.org/10.1016/j.ecolind.2023.110928
Received 1 June 2023; Received in revised form 9 August 2023; Accepted 6 September 2023
Available online 19 September 2023

1. Introduction

Urban areas are hotspots of human housing and activities and currently host about half of the world's population; global urbanisation is still ongoing, with growth prospects estimating that, by 2050, 70% of people will live in cities (The World Bank, 2022). Although covering around 3% of the global land, urban areas are responsible for >70% of CO_2 emissions (Wu et al., 2020), thus exacerbating the ongoing climate change. Urbanisation is generally associated with the alteration of the energy budget and modifications to the biogeochemical and water cycles, as well as the emission of pollutants in soil, water, and atmosphere (Grimm et al., 2008; Semeraro et al., 2021). As a result, urban living conditions often include air pollution, heatwaves, floods, and noise pollution (Morillas et al., 2018; Raymond et al., 2017), which are all considered to be a massive threat to human health and well-being.

More specifically, air pollution caused by domestic heating, vehicular traffic, and other anthropogenic activities is considered the largest environmental health risk factor in Europe (EEA, 2022). The urban environment promotes the formation of primary and secondary air pollutants such as PM_{10}, NO_2 and O_3 (Krzyzanowski et al., 2014; Sicard et al., 2018), which exert a remarkable impact on human health by causing and aggravating respiratory and cardiovascular diseases (EEA, 2022). To properly face the hazard of pollution, the EU has launched the Zero pollution action plan (European Commission, 2021), with the ambitious goal, amongst others, of improving air quality and reducing by 55% the number of premature deaths attributed to air pollution before 2030.

Air pollution is critical in Italy as well. Currently, for PM_{10}, $PM_{2.5}$ and NO_2, only a few Italian-monitored cities comply with the World Health Organization (WHO) threshold values for human health protection (Legambiente, 2022). Despite being traditionally depicted as a pollutant with a rural character (Gerosa et al., 2009), O_3 will likely acquire an increasingly urban connotation under current climate projections. Many tree species commonly used for urban greening emit substantial amounts of Biogenic Volatile Organic Compounds (BVOCs) that are known for their potential to act as O_3 precursors, and whose emission is positively correlated to temperature (Chen et al., 2020). The progressive warming of urban areas (i.e. urban heat islands) may then cause a larger relative increase in O_3 concentrations in cities (Sarrat et al., 2006). This effect may further be reinforced by the successful implementation of policies aimed at reducing pollutant concentrations, especially NO_x, in urban areas, so that the ozone chemistry in this context will become increasingly regulated by BVOCs emissions (Fitzky et al., 2019).

For Italy, in terms of air quality, there is a clear distinction between the Po Valley plain and the rest of the territory. The Po Valley, an alluvial plain that covers most of northern Italy, has widely been recognized as one of the most polluted regions of Europe throughout all year (Filippini et al., 2021; EEA, 2022), both for the presence of highly developed industrial and agricultural areas, and unfavourable weather and climatic conditions that promote the air pollutants' accumulation (Diémoz et al., 2019). Otherwise, in central and southern Italy, cities are more exposed to high solar radiation that in turn promotes photochemical smog; however, air pollution is generally not exacerbated by any specific adverse condition (Legambiente, 2022). For Italy, PM and O_3 were responsible for 52,000 and 6,000 premature deaths respectively for the year 2020, which is more than any other European country (EEA, 2022).

Nature-Based Solutions (NBSs), i.e., solutions inspired by the functioning of ecosystems and supported by them, represent a viable tool for the sustainable management of cities. NBSs take advantage of the high efficiency of natural processes to provide societal and environmental benefits (Cohen-Shacham et al., 2016; Orioli et al., n.d) and are increasingly used to address the environmental criticalities of urban areas (Raymond et al., 2017). Urban Green Infrastructure (UGI), that is, urban and *peri*-urban forests, hedges, and street trees, falls under the umbrella of the NBSs and may help address the above-mentioned challenges by providing multiple Ecosystem Services (ESs), such as PM_{10} and O_3 removal from the atmosphere and extreme summer temperature mitigation (Fares et al., 2020; Manes et al., 2016, 2012; Marando et al., 2019). Enhancing the environmental quality of cities and promoting human health and urban regeneration through NBSs is nowadays a well-established priority of the global political agenda. Goal 11 of the United Nations (UN) 2030 Agenda for Sustainable Development (United Nations, 2015) explicitly remarks the need for more high-quality and accessible public green spaces in cities; the EU Biodiversity Strategy for 2030 (European Commission, 2020) sets the goal of planting at least 3 billion trees in the EU by 2030, and calls all cities with at least 20,000 inhabitants to develop an ambitious greening plan In Italy, with the National Recovery and Resilience Plan (PNRR) funded by the Next Generation EU, a total of EUR 330 million were allocated to the "Urban and extra-urban forestry plan", which sets the goal of planting at least 6.6 million trees in 14 Metropolitan Cities by 2030.

In this framework, there is an urgent need for studies aimed at defining policy priorities and best management practices to properly establish the upcoming green areas and to fully exploit the associated ESs provision. To operationalise the ESs conceptual framework, a multidimensional analysis of the ecological and social context is required (Winkler et al., 2021). One way to carry out such an analysis consists of comparing the biophysical and spatial estimate of ESs provided by urban green, that is called the supply, with the demand, defined as the quality and quantity of services required by the society in that specific context (Villamagna et al., 2013). Once ESs supply and demand have been estimated, the ESs balance, that is the "difference between societal demand for ecosystem services and the capacity of ecosystems to provide these services in a sustainable manner" (Cumming et al., 2013), can be spatially defined. Eventually, mismatch areas, which are those showing unmet demand, should be set as priority areas for the implementation of interventions aimed at enhancing their sustainability (Baró et al., 2015; Sebastiani et al., 2021).

The ESs mismatch, which has often been associated with dense, highly populated urban areas (Baró et al., 2016; González-García et al., 2020), negatively affects the resilience of urban ecosystems, leading to poor environmental conditions and deteriorating the quality of life (McPhearson et al., 2022; Winkler et al., 2021). Depending on the ES, the mismatch is generally characterised by seasonal trends that should be addressed too (Schmalz et al., 2016). For example, PM_{10} pollution is generally relevant in winter, when phenomena such as domestic heating and thermal inversion take place, whereas O_3 concentrations are particularly worrying during summer, as these highly depend on the persistence of stable atmospheric conditions and solar radiation (European Environment Agency, 2018a). Despite the importance of the temporal dimension of supply and demand, this aspect has often been overlooked (Yao et al., 2021).

The objective of this study is to assess the ESs mismatch for air quality amelioration, intended as the abatement of O_3 and PM_{10} pollution, in four Italian Municipalities (Milan, Bologna, Rome, and Bari). Given the expected seasonality in ES provision, for O_3 and PM_{10} we quantified both the ES supply and demand in winter and summer respectively using a Composite-Indicator-based approach, and then combined these to evaluate mismatch areas in each Municipality. Based on this comprehensive index, priority areas could be proposed and indicators of mismatch at the city or national level pointed out.

2. Material and methods

2.1. Study area

The study was carried out in four Italian Municipalities located along a north-south gradient, to represent the urban diversity and the differential pollutant distribution along the Italian peninsula. For northern Italy, we selected Milan and Bologna; for central and southern Italy, we selected Rome and Bari respectively. Land Use and Land Cover (LULC)

classifications are reported in Fig. 1.

Milan (45° 28′ 38″ N, 9° 10′ 53″ E) is one of the largest Municipalities in northern Italy, spanning 181 km^2. It hosts 1.3 million inhabitants, with a mean population density of about 7566 in/km^2, peaking at around 12,000 in/km^2 at the city centre. The Municipality of Milan has a high degree of soil consumption, which equates to about 58% (ISPRA, 2022) of the total surface, whereas urban and *peri*-urban green areas cover about 8.7% (derived from Copernicus Land Monitoring Service, CLMS, Urban Atlas). Milan also displays a remarkable diversity of economic sector and a strong manufacturing industry (Armondi and Di Vita, 2017), and is considered one of, if not the most, economically developed cities in Italy (dell'Agnese and Anzoise, 2011).

Bologna (41° 7′ 7″ N, 16° 51′ 7″ E) lies on 141 km^2 and has a population of about 390,000 inhabitants; the population density is on average 2,779 in/km^2, with peaks of 11,000 in/km^2 at the city centre. The soil consumption is attested at 33.8% (ISPRA, 2022) of the total municipal surface, whereas green areas cover about 11% (derived from CLMS, Urban Atlas). Both Milan and Bologna are in the so-called Padana Plain, which is known for its extremely low air quality (Traversi et al., 2009).

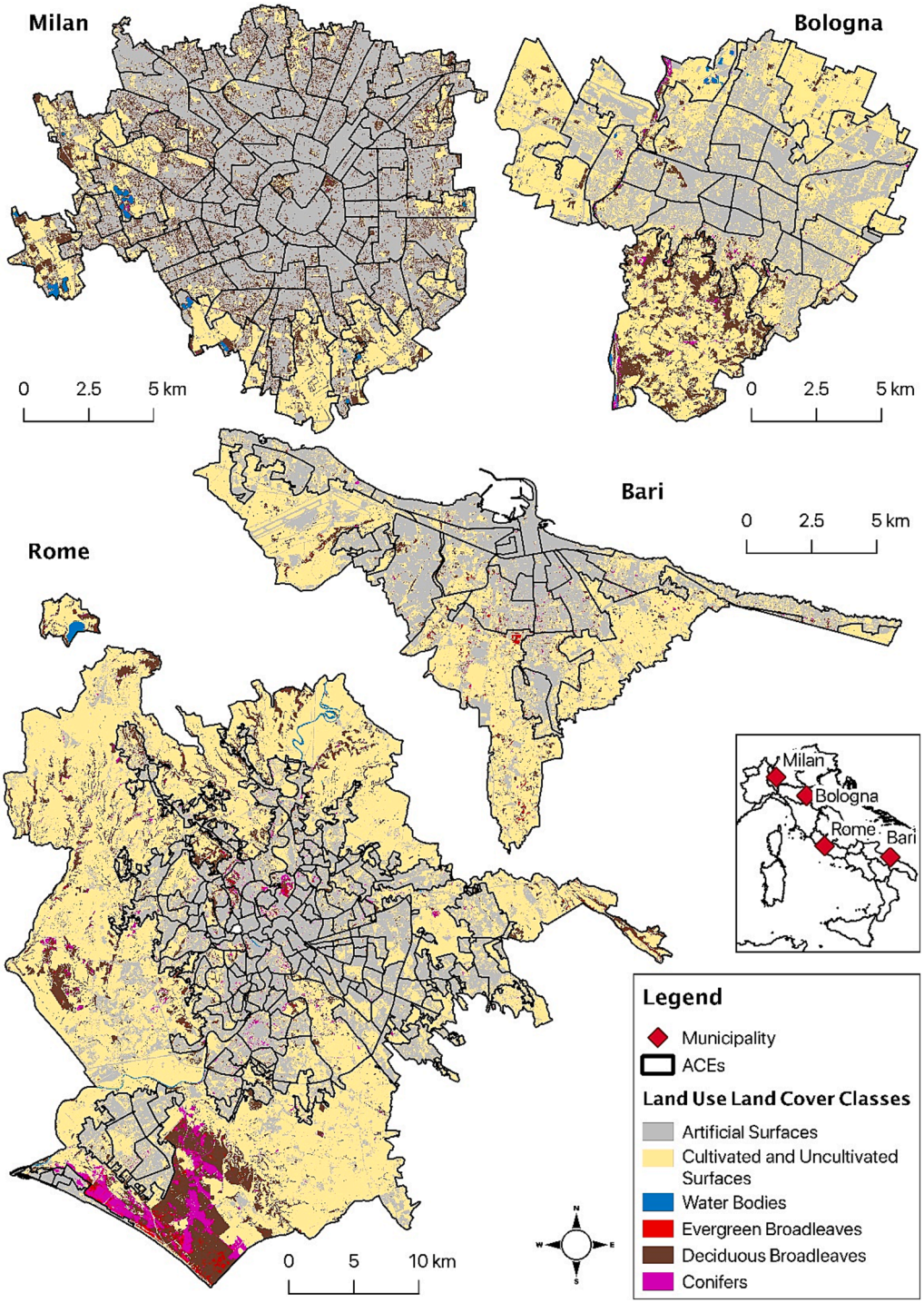

Fig. 1. Land Use and Land Cover classification for the four Municipalities. The black lines delineate the limits of Census Areas (ACEs), a common territorial base for data aggregation defined by ISTAT (Istituto Nazionale di Statistica).

Rome (41° 54′ 39″ N, 12° 28′ 54″ E) is the Italian Capital, and it's located in central Italy. It is by far the largest municipality of Italy, spanning 1,285 km^2; the urban core is about 25 km far from the Tyrrhenian coast. Rome hosts about 3 million dwellers, showing an average population density of around 2,200 in/km^2, with peaks of 9,000 in/km^2 in the city centre and lows of 1,000 in/km^2 in peripheral areas. Soil consumption is currently at 23.6% of the total municipal area (ISPRA, 2022); urban and *peri*-urban green areas occupy about 12% of the total surface.

Bari (41° 7′ 7″ N, 16° 51′ 7″ E) is situated in southern Italy, on the Adriatic coastline, occupying 117 km^2. It has a population of about 326,800 inhabitants, with a mean density of around 2,700 in/km^2. Soil consumption amounts to 43% of the total municipal surface, and urban green areas are very rare, covering about 1%, which is amongst the Italian lowest (Sanesi and Chiarello, 2006).

It's noteworthy that all 4 cities have a compact urban core characterised by high settlement concentration and population density, and several dispersed urban settlements towards the suburban areas (Salvati et al., 2018).

2.2. Selection of ES supply and demand indicators

We focused our attention on tropospheric ozone (O_3), which shows higher concentration during summer and is considered a threat to both human and environmental health (Karlsson et al., 2017), and Particulate Matter (PM), a typical winter pollutant that is mostly critical in northern Italy. Composite Indices (CIs) were used to quantify the supply and demand for O_3 and PM_{10} removal provided by vegetation; each CI resulted from the aggregation of multiple single indicators. Such an approach allows for summarising multidimensional phenomena (e.g. air pollution, population density and vulnerability, green cover) into one single numeric value without dropping any underlying information (The Organisation for Economic Co-Operation and Development (OECD) (2008)).

To adopt a coherent spatial unit among the four Municipalities, we used the Census Areas (ACEs) defined by ISTAT (Istituto Nazionale di Statistica) as the common territorial base for data aggregation (Fig. 1). ACEs provide a sub-municipal partition of the cities driven by infrastructural constraints (main roads, railways) and geographical barriers (rivers, canals, ridges, ditches), as well as demographic and social data. Each ACE has a population ranging from 13,000 to 18,000 citizens. The ACE 0 refers to the non-contiguous residual parts of the municipal territory where population densities are generally low. Therefore, CIs were calculated at the ACE scale. For an exact representation of ACEs' boundary and numbering refer to the Supplementary Material (Figs. S1 and S2).

To build the CIs we first defined a theoretical framework that allowed us to select several relevant indicators.

To compose the Supply Index (SIi) we used the formula illustrated in Eq. (1).

$$SIi = \frac{Vp_i}{A_{ACEi}} \quad (1)$$

Vp_i is the vegetation potential to adsorb pollutants (O_3 and PM_{10} expressed in Mg*y^{-1}) in each ACEi; A_{ACEi} is the area of the corresponding ACEi (expressed in ha). Vp_i for O_3 removal was computed following the approach adopted by Manes et al. (2012), which uses Land Cover data as well as data of the stomatal conductance of different Functional Groups of vegetation and the length of the photoperiod. Vp_i for the PM_{10} removal was estimated using a removal model first proposed by (Nowak, 1994), and subsequently re-adapted by Manes et al. (2016), which integrates Land Cover data, Leaf Area Index (LAI, m^{2}m^{-2}), deposition velocity of PM, and information on the phenology of different Functional Groups of vegetation. The Land Use Land Cover (LULC) maps (spatial resolution of 10 m) for the four Municipalities were obtained through a supervised classification; a detailed review of the classification process and a description of the classification accuracy assessment are presented in paragraph 2.3. Mean seasonal LAI data from winter 2019 (spatial resolution of approximately 300 m) was obtained from the Copernicus Global Land Service) database. Following Sebastiani et al. (2021) we ran the model simulating a uniform pollutant concentration of 1 μg/m^3 for the entire study area (both for O_3 and PM_{10}), thus providing a measure of the potential of vegetation (Vp_i) to ameliorate air quality under homogeneous pollution conditions.

The models used to derive the O_3 and PM_{10} removal potentials were implemented in GRASS GIS using a spatially explicit approach that allowed for the reaggregation of output data according to the chosen territorial base (ACEs). More details relative to the models are reported in the Table S3 of Supplementary Materials.

The Demand Index (DI) integrates two dimensions: the first one is related to the population exposure to the target pollutant, described by the average seasonal pollutant concentration and the population density; the other includes a measure of the population's vulnerability. To compute the latest, we assumed the vulnerable population to be composed of the elderly (>65 years) and young people (<10 years), as both categories are at greater risk of the adverse health effects given by excessive pollution exposure (Combes and Franchineau, 2019; Mudway et al., 2019). We integrated the two indicators using a simple linear combination method (The Organisation for Economic Co-Operation and Development (OECD) (2008)); before the aggregation, which is presented in Eq. (2), both terms were re-scaled on a range from 0 to 100 using the min-max procedure.

$$DIi = \frac{[C]i + (d_{popi} * fv_i)}{2} \quad (2)$$

Here, [C]i refers to the normalised average winter and summer concentrations (μg/m^3) for O_3 and PM_{10} respectively in each ACEi, obtained from integrated air quality modelling systems provided by the Regional Environmental Protection Agency (ARPA). We decided to carry out elaborations on different single-seasonal bases, as the two pollutants display a marked seasonality that heavily influences their impact on public health at two different moments of the year. Data on population density (d_{popi}, in/ha) and population vulnerability (fv_i) were obtained from ISTAT and aggregated at the ACE level.

For better comparability, SIi and DIi were normalised according to the min-max procedure and then converted into a range from 0 to 100, following Eq. (3):

$$Xi = \frac{xi + min(x)}{max(x) - min(x)} * 100 \quad (3)$$

where *xi* refers to a generic variable that changes along with index i, and *Xi* its corresponding normalised value.

2.3. Land Use Land Cover classification and accuracy assessment

The LULC maps for the four Municipalities were obtained through a supervised classification performed using Sentinel-2 level 2A products (S2MSI2A) from the summers of 2016 and 2019. The S2MSI2A product provides atmospherically corrected surface reflectances; tiles are delivered in cartographic geometry. The satellite images were processed using the open-source SeNtinel Application Platform (SNAP), Sentinel-2 toolbox, distributed by ESA/ESRIN (European Space Agency (ESA) (2015)). S2MSI2A product bands were resampled to a spatial resolution of 10 m.

Using the available LULC and vegetation maps such as Corine Land Cover 2018 (European Environment Agency, 2018b) and *Carta della Natura* (Casella et al., 2008; Angelini et al., 2012; Cardillo et al., 2021) as reference products, Regions Of Interests (ROIs) were collected for each LULC class; the average spectral signature was calculated to train a Maximum Likelihood Algorithm. Six LULC classes were identified: artificial surfaces, cultivated and uncultivated land (including pastures,

bare land or sparsely vegetated areas), water bodies, and three Functional Groups of vegetation – evergreen broadleaves, deciduous broadleaves, and conifers. Given the intrinsic heterogeneity exhibited by the artificial surfaces' reflectance, which makes the classification process rather cumbersome, and the interest in focusing on green cover for ESs assessment, the class of artificial surfaces was obtained from a national land consumption cartography published by the Italian Institute for Environmental Protection and Research in 2019 (ISPRA, 2021), which mapped impervious surfaces with a geometric resolution of 10 m, through photointerpretation of S2 imagery and ground-validation. The LULC classifications retained the S2MSIL2A product's spatial resolution of 10 m.

Each classification was evaluated through an accuracy assessment. Following Oloffson et al. (2014), we derived the total number of training samples (N) for the collection of ground-truth data as follows:

$$N = \left[\frac{\sum_1^c (W_i * S_i)}{S_0}\right]^2 \quad (4)$$

W_i is the mapped area proportion of LULC class *i*, which is derived directly from the classification; S_i is the standard deviation of stratum *i*; c is the total number of classes; S_0 is the expected standard deviation of overall accuracy. S_i were calculated following Cochran (1977):

$$S_i = \sqrt{U_i(1-U_i)} \quad (5)$$

where U_i refers to the user accuracy (defined as the proportion of correctly mapped area of class *i* to the total area mapped as class *i*). We assumed a minimum acceptable U_i of 0.8 (80% user accuracy), whereby we obtained $S_i = 0.4$ for all classes in the four Municipalities, and an expected S_0 of 0.01 following Congedo (2021). To stratify the sample proportionally to the relative area of each class in the four Municipalities, while also allocating an adequate number of Training Samples (N_i) to those classes with a limited surface (e.g. green cover), we calculated N_i as the average between estimates provided by assuming an equal distribution (6) and a weighted distribution (7).

$$N_i = \frac{N}{c} \quad (6)$$

$$N_i = N * W_i \quad (7)$$

Training samples were randomly generated and distributed using the Semi-automatic Classification Plug-in (SCP) available for the open-source software QGIS. Based on reference maps and photointerpretation, each training sample was assigned to a class. Through the accuracy assessment function provided by SCP, several accuracy statistics were calculated, including overall accuracy, user accuracy, producer accuracy and Kappa hat (Congedo, 2021). Overall accuracy proved in all cases to be above 80%, which is commonly interpreted as an acceptable measure (Anderson et al., 1976). Details on the specific sample design implemented for each Municipality, error matrices the accuracy statistics are provided as Supplementary Material (Tables S4 – 11).

2.4. Evaluation of Ecosystem Services' mismatch

The evaluation of the Ecological Supply-Demand Mismatch (ESDM) allows for a direct comparison between the ecological function (supply) and the human demand and may help identify areas with an ES provision deficit or surplus. The ESDM for each ES has been calculated as follows:

$$ESDMi = SIi - DIi \quad (8)$$

where SIi and DIi refer to the normalised Supply and Demand Indicator values of ACE_i. The ESDM provides an immediate interpretation of surplus (ESDM >0), balance (ESDM ≅ 0) and deficit (ESDM <0) in ES provision.

Finally, following Chen et al., (2019), we calculated the Comprehensive Ecosystem Supply-Demand Mismatch (CESDM) as the arithmetic mean of ESDM values obtained for the two ESs in each ACE:

$$CESDMi = \frac{1}{n}\sum_{j=1}^{n} ESDMi \quad (9)$$

where n is the number of ESs being analysed (in our case n = 2). The theoretical lower and upper limits of CESDM are therefore −100 (extreme mismatch for both ESs) and +100 (extreme surplus in both ESs). Subsequently, based on CESDM scores, we classified each ACE according to its ESs balance, applying the criteria reported in Table 1.

Table 1
ACE classification was applied depending on the Comprehensive Ecosystem Supply-Demand Mismatch (CESDM) score intervals.

CESDM intervals	ESs mismatch ranking
−100≤ CESDM ≤ −50	High deficit
−50 < CESDM ≤ −15	Moderate deficit
−15< CESDM ≤ 15	Balance
15< CESDM ≤50	Moderate surplus
50< CESDM ≤100	High surplus

2.5. Drivers of mismatch

We investigated the relationship between the CESDM and green cover for each ACE by using linear regression; we than explored the CESDM variability explained by green areas, structural and socioeconomic variables through the Principal Component Analysis (PCA). Linear Regression was performed in R-studio with Green Cover Percentage (GCP) as the independent variable, and CESDM as the response variable. GCP was calculated as the percent surface area covered by vegetated pixels in each ACE, as obtained in the LULC classifications illustrated in Fig. 1. Expecting a positive relationship between GCP and CESDM, we were interested in assessing how green space relates to achieving balance between ES supply and demand. Intersection between the fitted regression lines and the interval of balance (−15< CESDM ≤15) was thus evaluated, together with the level of significance in the regression. PCA is a technique that reduces the dimensionality of large datasets while retaining most of their variation (Jolliffe, 2005); therefore, it allows us to understand the main components able to explain the observed variability inside the dataset (Ringnér, 2008). We included the following variables in the analysis: percentage of high-density urban fabric (DU, %), percentage of medium-density urban fabric (MDU, %), buildings' height (BH, m), percentage of Urban and Peri-Urban forests (UPUF, %), distance from the city centre (DCC, km), distance from the closest green area (DGA, m), and average income (In, € y^{-1}). We plotted the ACEs according to PC1 and PC2, to better visualise the behaviour of the prior groups formed according to the CESDM score (see Table 1) concerning the selected variables.

DU, MDU, UPUF, and DGA were estimated using the Copernicus Urban Atlas database (European Environment Agency, 2018c); income was assessed using 2020 income declaration data collected and provided by the Department of Finance of the Italian Ministry of Economy and Finances.

3. Results

3.1. Evaluation of ES supply, demand, and mismatch

The four Municipalities show substantial differences in the supply of O_3 removal. Milan (Fig. 2A) strikes the attention since about 81% of the territory falls within the low supply interval (0≤ S ≤20) with the only exception of ACE 0 which is located in the external part of the Municipality (for further details about ACEs location refer to Fig. S1). The demand remains high mainly in the central quadrants of the city: 6% of the Municipality falls in the upper interval (80< D ≤100), whereas the

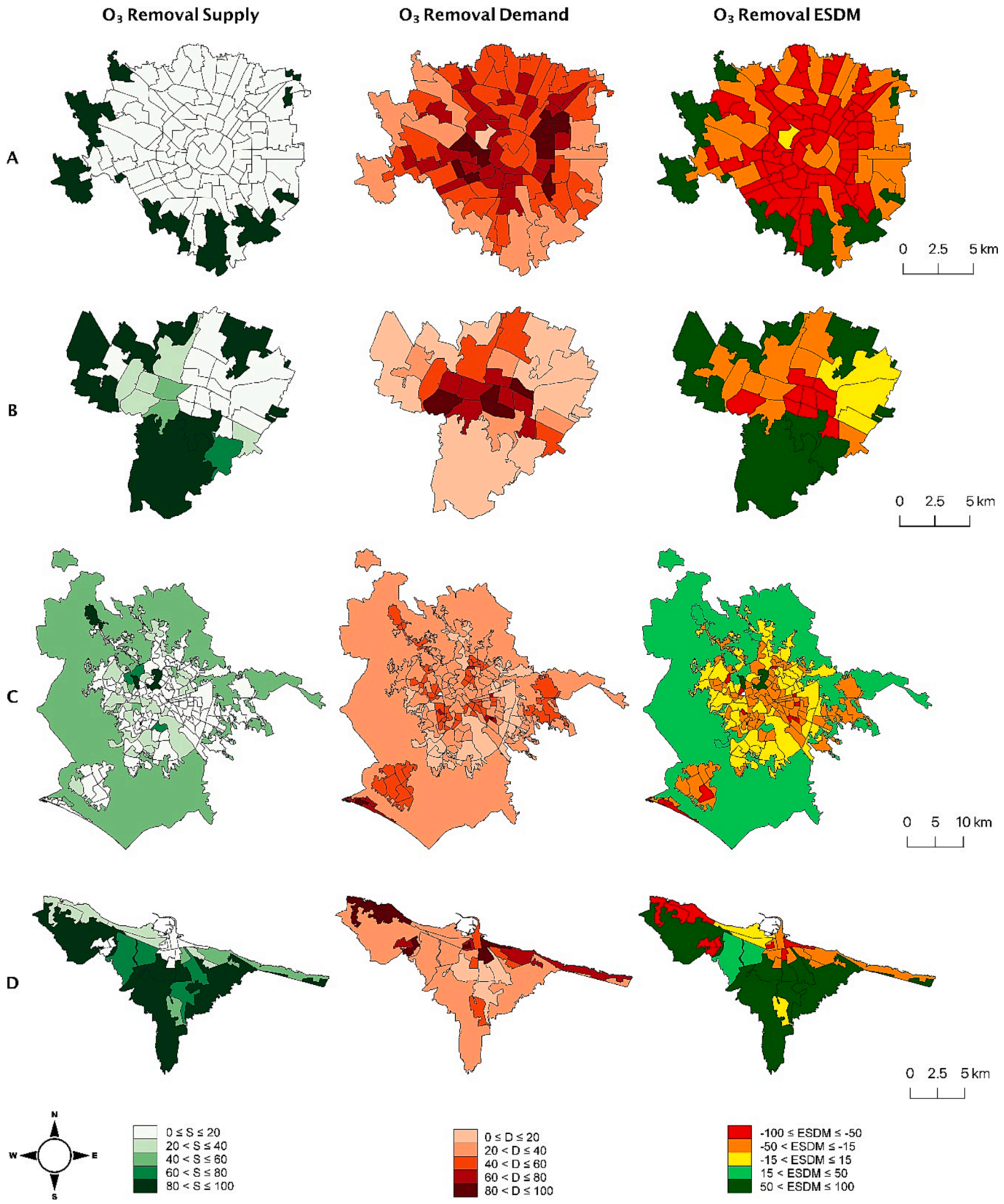

Fig. 2. Spatial distribution of the Supply, Demand and Ecological Supply-Demand Mismatch (ESDM) Indicators of O_3 removal in A) Milan; B) Bologna; C) Rome; D) Bari.

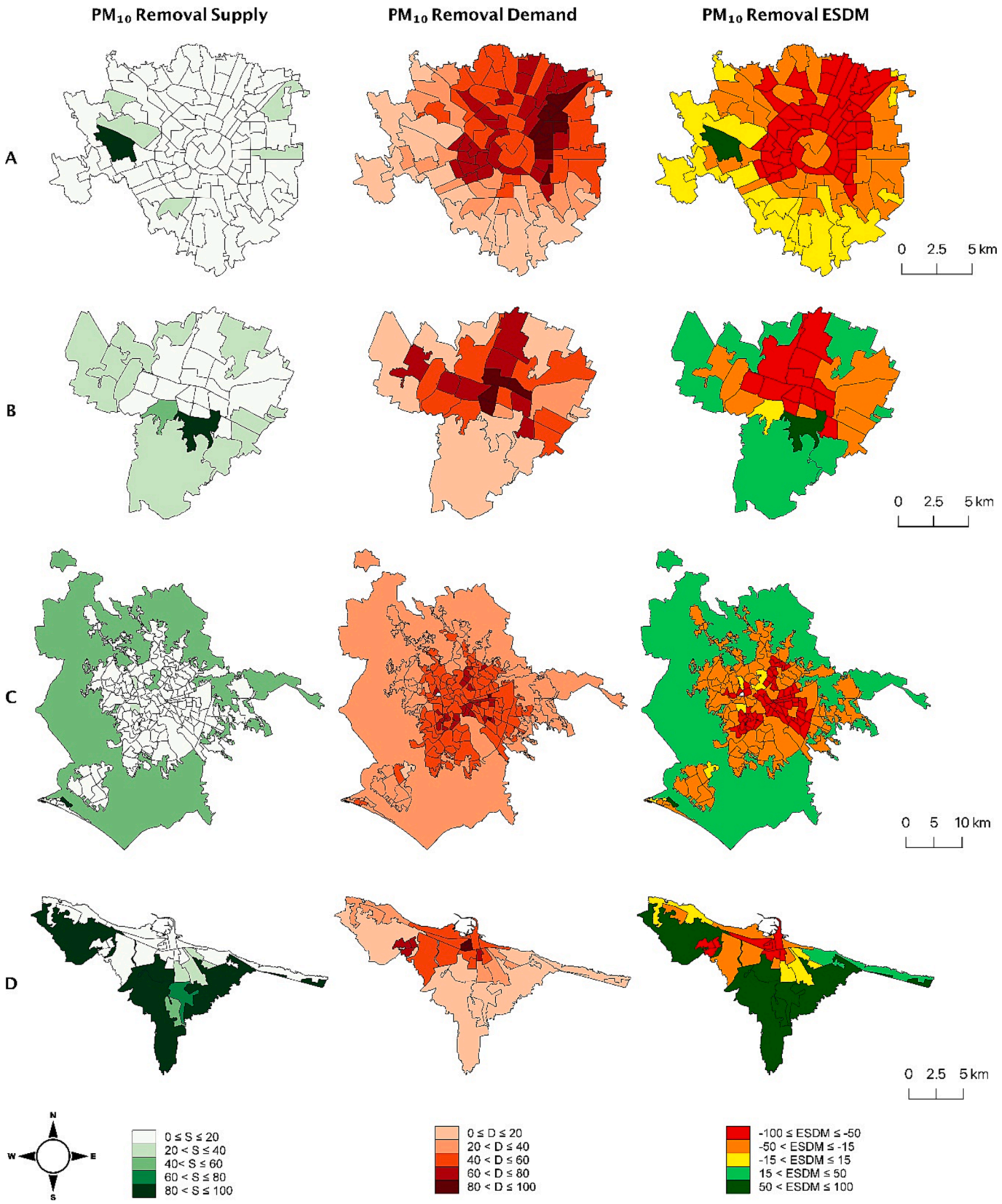

Fig. 3. Spatial distribution of the Supply, Demand and Ecological Supply-Demand Mismatch (ESDM) Indicators of PM_{10} removal in A) Milan; B) Bologna; C) Rome; D) Bari.

interval 60< D ≤80 includes around 19%. 40 % of the territory addresses the medium demand level and around 34% is ascribable to the lower interval (0≤ D ≤20), about half of which is represented by ACE 0. Accordingly, negative ESDM values for O_3, between −100≤ ESDM ≤ −15, were found throughout the city, especially in its central part. Only ACE 0 presented a positive value (S > D).

For PM_{10} removal (Fig. 3A), 88% of the municipality has a very low provisioning capacity (0≤ S ≤20) paired with high demand, especially in the central part and in the northeast quadrant of the city where 4% of ACEs fall in the high interval (80< D ≤100). The intermediate intervals 40< D ≤60, 60< D ≤80 are equally represented in the Municipality (~45%). It is interesting to notice that for PM_{10}, differently from what was found for O_3, the "green belt" included in the ACE 0 does not reach a complete positive balance (S > D).

For Bologna, relative to O_3 (Fig. 2B), 48% of the total Municipality falls in the high supply intervals (80< S ≤100), almost entirely determined by the presence of ACE 0 (45% of the territory), whereas the central ACEs, that fall into the low supply intervals, also shows a higher demand. This leads to a strong mismatch in the central part of the city (8% of the total extension) which decreases radially towards the periphery. The PM_{10} provisioning (Fig. 3B) presents a more critical situation since there is only one ACE associated with the higher supply, and 36% of the city belongs to 0≤ S ≤20 interval. The spatial trend of demand is quite similar between O_3 and PM_{10}, with a high level of demand concentrated in the city centre. Accordingly, the mismatch spatial pattern is quite superimposable between O_3 and PM_{10}, with some differences as only one ACE presents surplus for PM_{10} (only ACE 62, see S1); for O_3 and PM_{10} respectively 9% and 20% of the Municipality falls in the lowest ESDM interval (−100≤ ESDM ≤ −50).

A large portion of the Rome Municipality is characterised by the medium supply capacity interval (40< S ≤60) for O_3 removal (Fig. 2C), whereas the most urbanised areas (see Fig. 1) present scarce supply, thus falling in the lower two intervals. In particular, the city centre and the South-East quadrants show very low supply and the highest demand values. As for PM_{10} (Fig. 3C), 35% of the Municipality falls in the lower interval of supply, whereas the ACE 0, which covers 63% of the territory, falls into the 40< S ≤60 interval. The high demand is located in the ACEs positioned in the central and the South-East quadrants of the city. The mismatch highlights a different situation for O_3 and PM_{10}. For the former, about 60% of the 147 ACEs present a deficit, with 9% of ACEs in the worst interval (-100≤ ESDM ≤ −50). Those ACEs are located both in the centre area and also in Ostia, a neighbourhood in the South-west part of the municipality situated along the coast. ACEs that show a surplus (S > D) are partially located in the peripheral part, or in the proximity of urban green areas as the ACE 80 which is a large natural protected area (see Fig. S1). The mismatch for PM_{10} is more pronounced than for O_3, indeed, 92% of the ACEs present a deficit. Those ACEs are well represented in the Eastern part of the Municipality, but also in the centre and the north quadrants.

The Municipality of Bari has a good supply distribution in the peripheral areas for O_3 removal (Fig. 2D): 68% of the territory falls in 80< S ≤100 interval, even if it is important to underline that 49% of those high-supply areas are represented by ACE 0. Only a small central area falls in the 0≤ S ≤20 interval (7% of the municipality). On the demand side, there is a quite clear trend with 76% of the Municipality that falls in the lower demand classes. PM_{10} removal (Fig. 3D) is more critical compared to O_3. Indeed, apart from ACE 0, most of the ACEs both in peripheral and central areas fall in the lower class of supply (0≤ S ≤20). Instead, the demand for PM_{10} is lower relative to what has been found for O_3, with only 21% of Municipality included in the higher demand

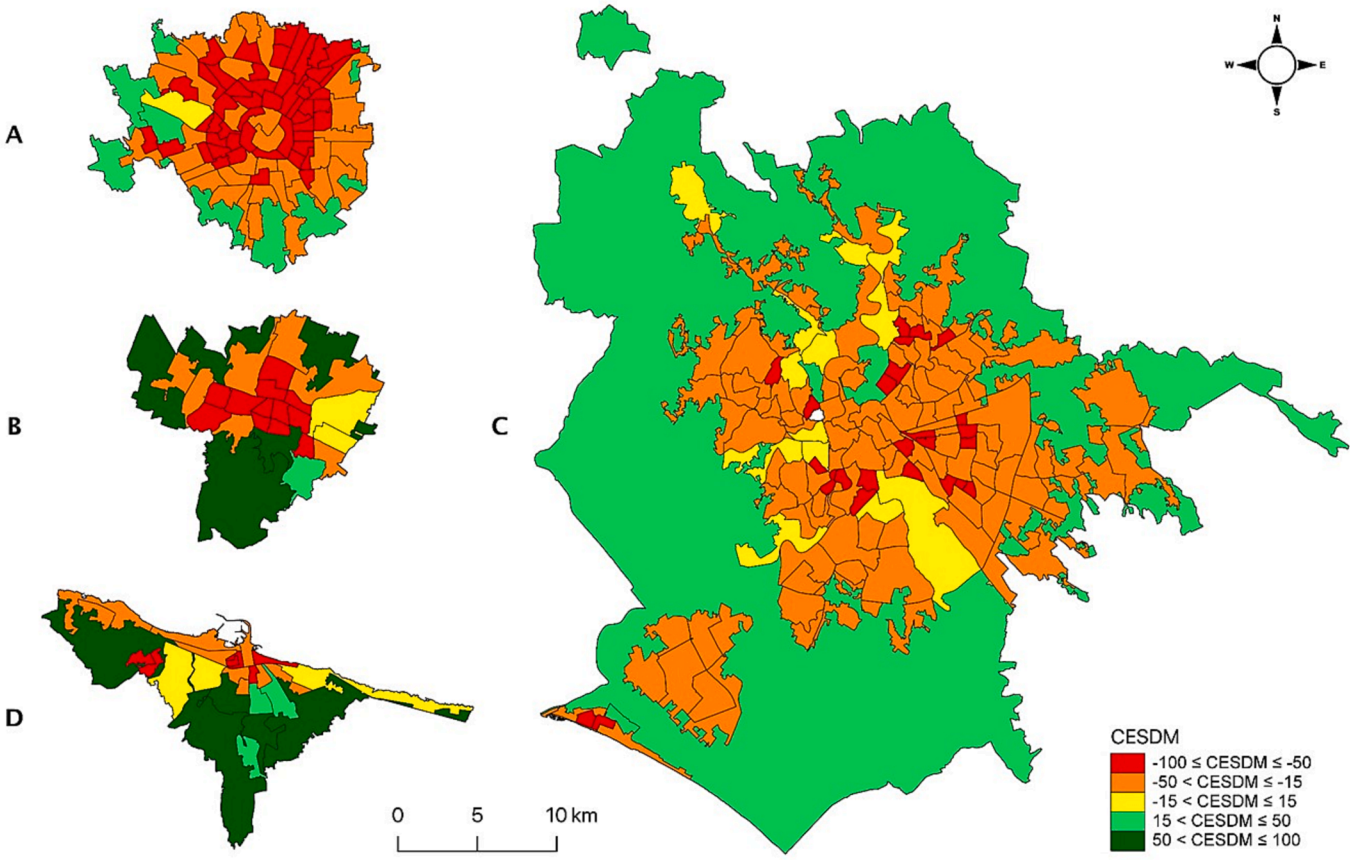

Fig. 4. Spatial distribution of the Comprehensive Ecosystem Supply-Demand Mismatch (CESDM) indicator in A) Milan, B) Bologna, C) Rome and D) Bari.

intervals. It is interesting to notice that in Bari the % of the territory included in high mismatch intervals (from −50< ESDM ≤ −15 up to −100< ESDM ≤ −50) does not differ too much between O_3 and PM_{10}, (around 22% for the former and 29% for the latter), but the spatial distribution and thus the more critical areas, are located differently. For O_3 the North-West area has higher mismatch; for PM_{10} the central one. However, for both pollutants, the more extensive part of the Municipality (ACE 0) falls in the surplus areas.

The comprehensive mismatch (CESDM) is shown in Fig. 4. In Milan (Fig. 4A), deficit areas are prevalent, with about 75% of the territory experiencing moderate to high mismatch, concentrated in two main quadrants of the city (i.e. North-East, South-West). It is interesting to notice the tight contiguity of ACEs presenting the highest deficit. This spatial pattern is present in Bologna too (Fig. 4B), where the higher deficit is localised mostly in the central areas and covers about 40% of the territory. In Rome moderate and high deficit areas outnumber surplus ones. 17% of the 147 ACEs fall in the high deficit interval (−100≤ CESDM ≤ −50) whereas only the 8% and 2% fall in the balance or moderate surplus intervals respectively. As for Bari, coastal areas present a high deficit and the peripheral ACEs show a surplus; around the 18% of the Municipality falls in the high/moderate deficit and balance intervals.

3.2. Drivers of spatial mismatch

Fig. 5 reports the relation between the Green Cover Percentage (GCP) for each ACE and the CESDM, showingfour distinct trends. As expected, in all Municipalities we found a positive correlation between GCP and CESDM, although R^2 varies remarkably. In Milan, GCP values are distributed over a large interval (0–29.2%), while CESDM values are mostly concentrated below the balance interval. There is a considerable variation in the data that is not explained by the regression model, as highlighted by R^2, which is rather low (0.33), especially if compared to the other Municipalities. Empirically, balance is found for ACEs with GCP values around 20%; however, the regression model indicates that balance is reached at 32%. In Bologna, GCP varies in the 0–17.3% interval, while CESDM values span most of the range (from −89 to 85). Most of the variability in the data is explained by the regression model (R^2 = 0.79). The difference between the empirical (2%) and the modelled (6%) values of GCP that satisfy a condition of balance is not as large as in Milan. In Rome, the range for GCP and CESDM is very similar to Milan (0–29.4% and −100 – 32 respectively). As opposed to the latter, although most ACEs have a GCP <10% and their respective CESDM values fall below the balance line, there is a conspicuous number of ACEs that are in a condition of balance. With the majority of the variability in the data explained by the regression model (R^2 = 0.61), the empirical versus fitted balance is found at around 5% and 10% respectively. Lastly, Bari is the municipality with the narrowest domain and the smallest GCP values (0–6.6%). The regression model predicts well the observed data (R^2 = 0.89). Empirical and modelled balance is found for GCP equal to 3% circa (Table 2).

Fig. 6 shows PCA's biplot for all of the municipalities. The ACEs clustered by high mismatch for air quality are located along a continuous gradient, PC1, that could be linked to the urban structure, as it shows increasing building height and share of the dense urban fabric. Throughout all cities, the ACEs in Balance, Moderate and High surplus conditions have higher scores on PC2, which is instead linked to the abundance of urban green areas. Medium-density built-up areas and Income fall in the third axis, which explains about 10–15 % of the variance in Milan and Rome, whereas in Bari and Bologna it is mostly represented by Income. It is interesting to notice that for all case studies the variance is explained by the same factors except for Bologna, in which the distance from green areas (DGA) contributes to positive CESDM.

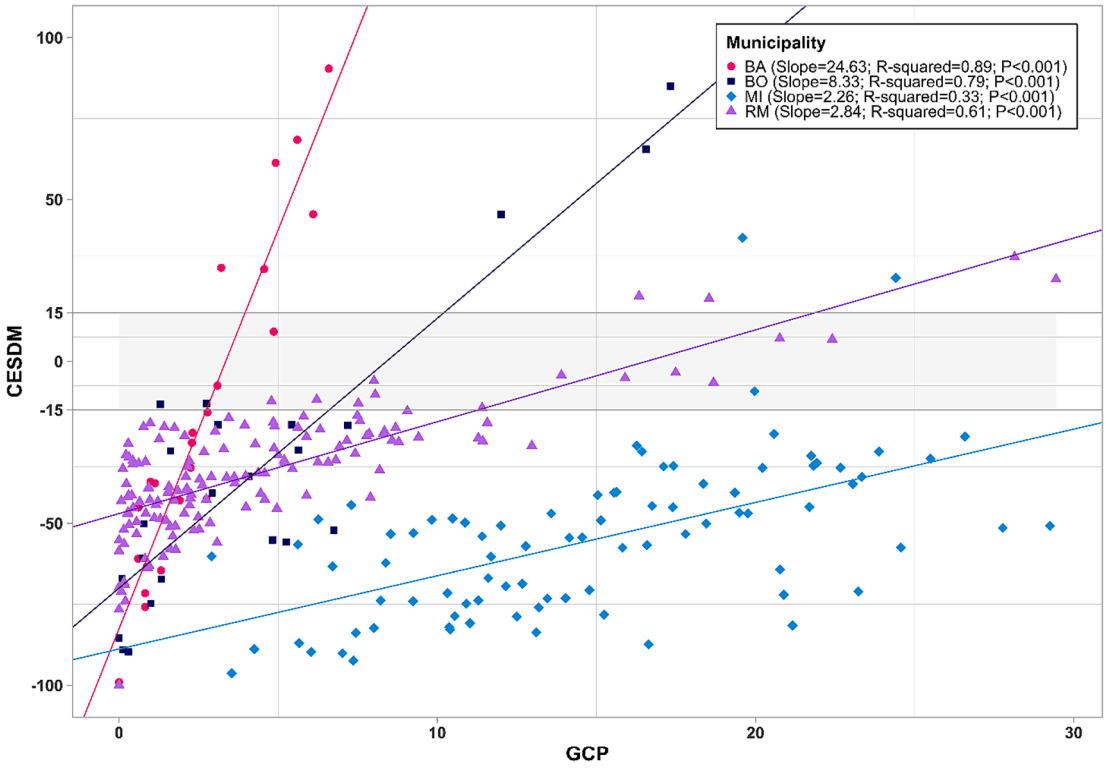

Fig. 5. Relation between Green Cover Percentage (GCP) on comprehensive supply–demand mismatch (CESDM) for each ACE in the four Municipalities. Regression analysis was applied and the output was reported in the inset. The grey band indicates the balance between supply and demand (- 15 < CESDM ≤ 15). (For interpretation of the references to colour in this figure legend, the reader is referred to the web version of this article.)

Table 2
Factor loadings of PCA of the four studied municipalities. Significant loadings (>0.33) are highlighted in bold. List of abbreviations: urban structure: distance from city centre (DCC, km) buildings height (BH, m), dense urban, (DU,%), medium-dense urban (MDU, %), distance from a green area (DGA, m); ecological and economic features: urban and *peri*-urban forest (UPUF, %), income (In, € y-1).

Milan	PC1	PC2	PC3	Bologna	PC1	PC2	PC3
DCC	**0.454**	−0.204	0.156	DCC	**0.514**	0.076	0.016
DGA	−0.160	**−0.686**	−0.284	DGA	0.205	**0.554**	**0.429**
BH	**−0.485**	0.170	−0.059	BH	**−0.544**	0.079	0.004
In	−0.388	0.322	**−0.486**	In	−0.262	−0.283	**0.865**
DU	−0.435	0.052	0.307	DU	**−0.529**	0.021	−0.256
MDU	0.345	0.165	**−0.725**	MDU	0.151	**−0.541**	−0.040
UPUF	0.273	**0.570**	0.187	UPUF	0.165	**−0.554**	0.019
Total Variance	53.92	20.78	9.73	*Total Variance*	44.96	31.19	11.45
Cumulative	53.92	74.70	84.43	*Cumulative*	44.96	76.15	87.60

Rome	PC1	PC2	PC3	**Bari**	PC1	PC2	PC3
DCC	**0.426**	−0.154	0.054	DCC	**0.471**	−0.047	0.178
DGA	0.278	**−0.506**	−0.134	DGA	**0.396**	0.429	−0.203
BH	**−0.564**	−0.173	−0.189	BH	**−0.468**	0.321	−0.180
In	−0.304	0.315	**−0.637**	In	−0.256	−0.281	**−0.781**
DU	**−0.446**	**−0.390**	0.108	DU	**−0.380**	**0.330**	0.195
MDU	**0.364**	0.114	**−0.639**	MDU	**0.358**	−0.305	**−0.343**
UPUF	−0.016	**0.652**	0.342	UPUF	−0.252	−0.655	**0.360**
Total Variance	36.44	24.26	14.23	*Total Variance*	47.52	19.28	14.48
Cumulative	36.44	60.70	74.93	*Cumulative*	47.52	66.79	81.27

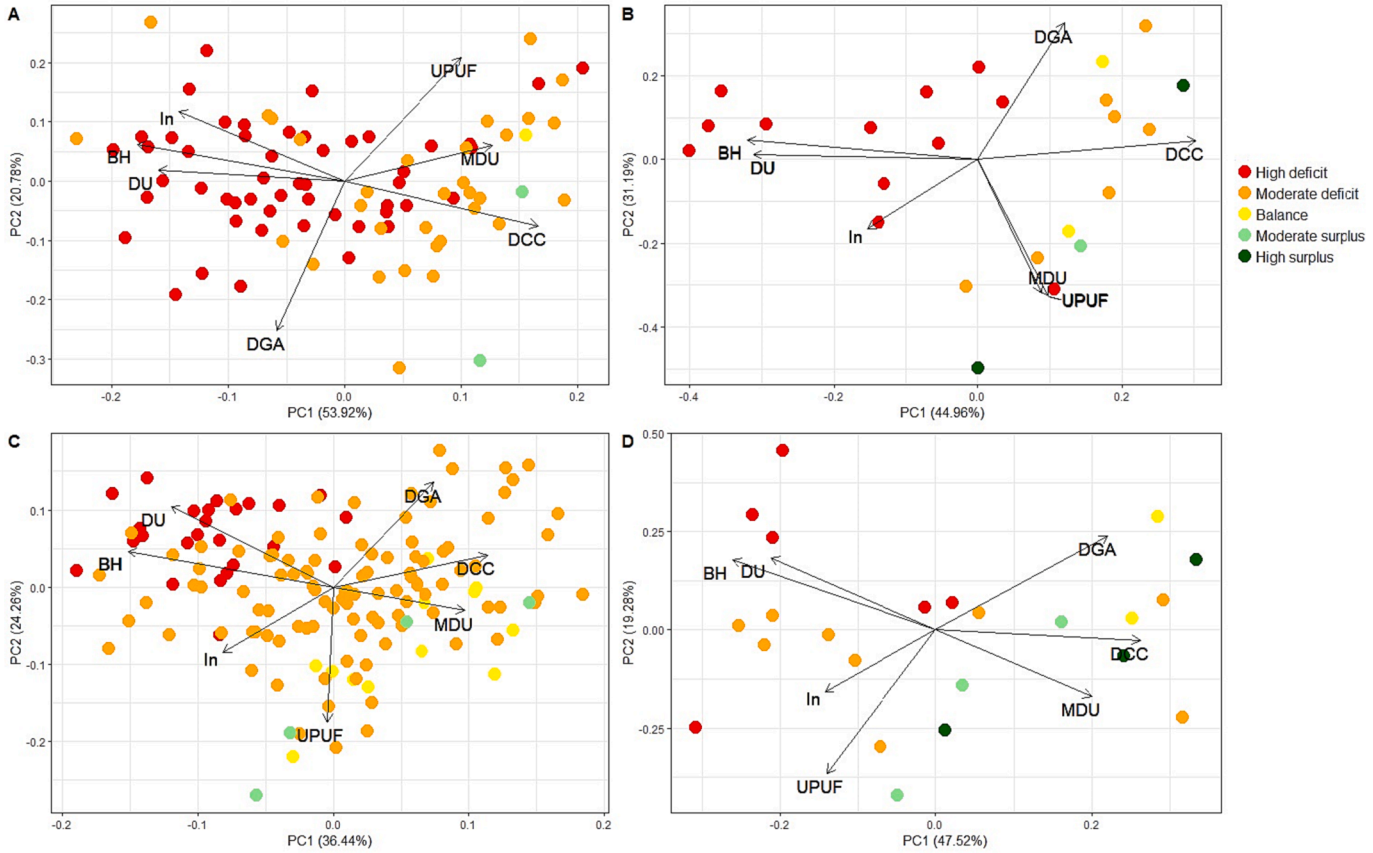

Fig. 6. PCA of the four Municipalities (A: Milan; B: Bologna; C: Rome; D: Bari) based on **urban structure:** distance from city centre (DCC, km) buildings height (BH, m), dense urban, (DU,%), medium-dense urban (MDU, %), distance from a green area (DGA, m); **ecological and economic features**: urban and *peri*-urban forest (UPUF, %), income (In, € y^{-1}). Each dot represents an ACE; colours refer to the overall mismatch condition (CESDM). (For interpretation of the references to colour in this figure legend, the reader is referred to the web version of this article.)

4. Discussion

4.1. City-specific features that affect the mismatch of ES

ESs supply and demand perspective can be a key means to implement sustainable land management strategies based on mismatch analysis. In this study, we analysed four Italian Municipalities as case studies to identify mismatch areas for air quality amelioration services, considering the seasonality of the selected air pollutants. The investigated Municipalities have different size, geographical location, historical backgrounds and urban planning traditions that resulted in a different rate of urban expansion (Zambon and Salvati, 2019). Milan experienced the highest mismatch among the four-study cases due to generalised low supply, especially for PM_{10} removal. Indeed, the removal of such a pollutant largely relies on evergreen tree species (Manes et al., 2014), which are rare in Milan, covering only 0.6% of the green areas in the Municipality. For management purposes, to enhance the PM_{10} removal potential, upcoming forestation practices should therefore aim at incrementing evergreen broadleaf species. Moreover, investing in these species that are constitutively more tolerant to oxidative stressors (Bussotti, 2008; Fusaro et al., 2021) represents an improvement in developing NBSs resistant and resilient to global change, also owing to the worsening scenarios forecasted by the IPCC (IPCC, 2023).

The supply capacity should be enhanced as a priority in the northeast and southwest quadrants, where the demand is higher. As highlighted by the relation between GCP and CESDM, which can help to disentangle the effects of unsatisfactory supply or high demand, UGI should cover at least 30% of each ACE to equilibrate the deficit of ESs provisioning. The harsh mismatch can be linked to high pollutant concentrations in both winter and summer and population density, which contribute to building a high demand. It is interesting to notice that, unlike other case studies where the city centre coincides with a high mismatch (Baró et al., 2015; Sebastiani et al., 2021; Shi et al., 2020), this doesn't happen in Milan. This evidence can depend on the positive effects that the restrictions on the circulation of the most polluting car types, which entered into force for the first time in 2012 and recently implemented, have on air quality. Thus, besides the UGI, the Municipality of Milan underlined that investments in new solutions for the mitigation of air pollution are also crucial.

In terms of PM_{10} removal, Bologna has a similar pattern to Milan, showing a higher mismatch relative to what surfaced for O_3 removal. Indeed also in Bologna the evergreen functional group is very underrepresented, whereas deciduous species, which play a key role in O_3 removal (Fares et al., 2020; Manes et al., 2016) are abundant, especially in the southern quadrant. Comparing our results with Vignoli et al. (2021), who considered annual PM_{10} removal and found a strong negative mismatch only for some of the central ACEs (no. 73, 7, 81, and 6, see Fig. S1), our findings highlighted that several other adjacent ACEs suffer from a similar condition. It is likely that, given the focus on the seasonality exhibited by the pollutants, our study highlights critical aspects derived from successive and prolonged events of low air quality.

As expected, the mismatch analysis for the Southern Municipalities, namely Rome and Bari, highlights several differences relative to the other two case studies in the distribution of high deficit intervals of mismatch and their frequencies. As for Rome, Sebastiani et al. (2021), showed that the mismatch in PM_{10} removal was worse in the eastern and southern sectors of the Municipality, characterised by a high degree of urbanisation. Our work confirms this pattern also for O_3. Indeed, most of the ACEs found to be in a high deficit condition ($-100 \leq$ CESDM ≤ -50) are situated in the eastern and southern quadrants, which combine a very low ES supply capacity with a higher demand. Green cover in these areas is extremely limited, while population densities and pollutant concentrations are the city's worst. However, as highlighted by the relationship between GCP and CESDM, the mismatch is expected to reach a balance or slight surplus at GCP >10%. Moreover, our findings in the case study of Rome highlighted substantial dispersion, and even for low GCP percentage, the CESDM is close to the balance (Fig. 5). This evidence might suggest the need to establish functionally diverse green areas, which stabilises pollutant removal throughout the year and across different environmental conditions playing a crucial role in delivering ESs (Wood and Dupras, 2021), where native adapted evergreen vegetation can thrive and guarantee the continuous provision of ESs throughout the year (Salvatori et al., 2016). Of great concern is also the occurrence of climate-change-driven biotic and abiotic stressors which affect the most common tree species in the Municipality (i.e. Stone pines, Holm oaks and palms) which are rapidly reducing the vitality of large green areas (Zappitelli et al., 2023). This is particularly important in southern Europe, which is expected to experience pronounced changes in climate over the next few years, with local projections for Rome predicting a mean annual temperature increase of 2–6 °C by the end of the century based on the business as usual scenarios (CMCC, 2022). Bari has by far the least share of green areas among the four Municipalities, with <9 m^2/inhabitant. Nonetheless, despite the low supply potential, the deficit looks moderate (Fig. 2C, Fig. 3C, and Fig. 4), which can be explained by low demand. Indeed, pollutant concentration is moderate for both O_3 and PM_{10}, and even if the population density is in the range of medium cities in Italy (ISTAT, 2020), the proportion of the vulnerable population is lower than elsewhere, slightly exceeding 30% in half of the ACEs, against the 80% found for Milan and Bologna, and the 60% for Rome. The scarcity of green areas also explains the steep slope of the regression line in Fig. 5, and suggests that the implementation of relatively small UGI (e.g UGI covers at least 5% of each ACE) may provide a huge contribution in filling the ESs deficit. In Italy, by 2050, the portion of the fragile population, namely people aged 65 and over, could represent 34.9% of the total population (ISTAT, 2022), requesting higher efforts to improve air quality since air pollution is more harmful to vulnerable subjects such as the elderly people or pre-adolescent children (Combes and Franchineau, 2019; Tétreault et al., 2016).

4.2. Urban patterns as indicators of intervention priority

Urbanisation is a complex phenomenon that has implications for urban structure because of anthropic filters such as city size, population density as well as the age of the settlement, overall affecting the vegetation and it capacity to provide ESs according to geographic location (McDonald et al., 2020). The investigated Municipalities have different sizes, geographical positions, historical backgrounds and urban planning traditions that resulted in a different rate of urban expansion (Zambon and Salvati, 2019). However, there are some common urbanistic indicators that represent the main drivers of mismatch. Indeed, beyond the wide biodiversity present throughout the Italian territory (Blasi et al., 2017) and the large differences among the Municipalities we considered, PCA pointed out that a certain bundle of urban features is associated with a high deficit of ESs provisioning. The presence of a dense urban fabric and the increasing buildings' height are generally linked to a marked mismatch condition. These variables do generally show medium to high loadings, in most cases well above 0.33, for PC1. Hence, we can state that a greater degree of urbanisation, specifically the compact one supporting urban dwelling, is likely to be associated with ESs mismatch. Interestingly, this is true regardless of the city's dimension, as it happens for both large cities like Rome and Milan, and for much smaller ones like Bologna and Bari. From a wider perspective, our results are attributable to the urbanisation and suburbanization processes that took place in Mediterranean cities over the last century. Indeed, as reported by Salvati and Carlucci, (2015), Mediterranean cities have largely followed the monocentric growth model, which is associated with high settlement concentration and population density, and intense economic activities. Likewise other European urban contexts, this scheme generates spatial decoupling between areas with high ESs demand and those with high supply (González-García et al., 2020). Furthermore this scheme hardly fostered interventions aimed at

preserving the environmental quality of cities, such as devolving space for urban green areas (Tomson et al., 2021). However, enhancing the vegetated areas to meet ES demand is not practical for the compact city centres assessed in the present study, suggesting the urgency to reduce the demand through more effective air quality policies. Among urban structures, also the so-called urban sprawl, that has taken place in Mediterranean regions lately (Salvati and Carlucci, 2016), has favoured the ESs mismatch due to a decrease in ESs supply in areas with growing population (Dupras and Alam, 2015; Yuan et al., 2019). Therefore, a new urban growth model, able to increase the abundance of urban and *peri*-urban forests without disregarding the socio-economic needs of urban dwellers, should be adopted. Indeed, especially for Regulating ES, the presence of urban and *peri*-urban forests (UPUFs), as well as their proximity and accessibility, is considered to be a crucial factor in determining the ESs mismatch balance or surplus (Marando et al., 2019). Therefore, we can safely state that living outside the city centre, far from densely urbanised areas, is the most determining factor in shaping the ESs mismatch. In our case study, the percentage of UPUFs together with the distance from the closest green area (DGA), generally shows significant loadings on PC2, identified as the axis linked to "balance", "moderate surplus" and " high surplus" areas. It is interesting to notice that for Milan and Bologna UPUFs and DGA have a different impact in shaping the ESs mismatch compared to Rome and Bari. This result may represent a development pattern typical of northern cities, with pronounced urban sprawl related to industrial areas, and the central and southern urban areas, in which, as in the case of Rome, the periphery is mostly devoted to rural activities (Fig. 1). It should be pointed out that our study did not consider private gardens, which have proven to be important in the ESs delivery at the city scale (Balzan et al., 2021). Although quantitative analysis of the socio-economic distribution of ESs has been poorly addressed, a few pieces of evidence highlight that the environmental quality tends to decrease by social deprivation (Mullin et al., 2018). In our cases study income does not play a crucial role in explaining the mismatch distribution. Indeed income loadings for both PC1 and PC2, except for Milan, tend to be low and often below the 0.33 threshold.

5. Limitations and shortcomings

To provide a national perspective in the mismatch analysis, we had to adopt a common territorial base to retrieve and analyse the data consistently in the four Municipalities. We adopted ISTAT's ACEs, a national territory partition applied to the main urban areas, carried out on demographic principles that aggregate the rural areas of the Municipalities, where population densities are much lower than inside the urban core, into one single polygon (ACE 0), disproportionately larger than any other ACE. This technical aspect meant two things. On one hand, the spatial resolution of the data in the rural belts is very different from that of the urban core, ultimately conditioning the level of detail in the demand indices construction. Secondly, the clean-cut separation between the urban core and the *peri*-urban areas does not depict well how ES provision changes along the urban-rural gradient, and the buffering role that the urban-rural interface holds concerning ES provision, which is a relevant aspect for the spatial analysis of ES mismatch. The CESDM, an effective benchmark for representing complex issues, calculated as the arithmetic mean of ESDM of each ES (Chen et al., 2019), framing the ESs at the integral level, might assign different combinations of supply-demand to the same mismatch raking. Thus mapping mismatch through this complex index entails a thoughtful analysis of a single ESDM. When adopting this methodology, it is necessary to consider that the accuracy of the results can be subjected to uncertainty and flaws derived from raw input data and simplification of the modelled processes.

6. Conclusions

We explored the spatial distribution and seasonality of the main threats to air quality (O_3 and PM_{10}) in four Italian Municipalities, to operationalise the ESs mismatch framework. This approach has been applied to solve three main purposes:

1) Assess city-specific features that can act as drivers of ESs negative mismatch.
2) Highlight potential common indicators of mismatch across different municipalities.
3) Pinpoint priority areas concerning upcoming forestation strategies that will be implemented in the Italian urban areas over the next years.

The results show that the northern municipalities (Milan and Bologna) experienced the worst conditions, as most of their surface is included in "moderate" to "high deficit" areas due to a combination of high demand on the side of pollutants concentration, and moderate supply linked to low functional diversity. Bridging these results with the national urban forestation plan and the guidelines about the species recommended for forestation, we suggest in these areas investing efforts in planting evergreen species is essential. Beyond being effective to optimise the provisioning of air quality improvement, this functional group can be important to foster the continuous delivery of multiple Ecosystem Services such as climate regulation. On the other side, southern cities experience different situations: Rome is characterised by high mismatch areas concentrated in quadrants of the cities where the demand is high in terms of population density. Bari presents a different case among those analysed: both supply and demand are low, except for a higher concentration of fragile populations that build up the mismatch in several ACEs in the city centre. In this Municipality it will be crucial to take action to heavily implement the percentage of green space, which is among the lowest in Italy, through investments in Green Infrastructure. Combining different Functional Groups can guarantee optimal ESs supply and resilience to climate adverse conditions that are going to markedly affect southern Italy in the next future (Nardella et al., 2023). The multi-city approach can support addressing the intrinsic complexity of these issues to achieve the formulation of general guidelines for designing and managing urban spaces sustainably. With this in mind, the output of Principal Component Analysis (PCA) provides insights into general urban features that affect the mismatch of air quality. The degree of urbanisation and compact residential neighbourhoods are often associated with ESs mismatch, and both the presence and distance from the green spaces are crucial in providing air quality regulation. The required extent of each ACE's Green Cover ranges from approximately 5% in Bari to about 30% in Milan. Our study is the first comprehensive attempt to frame the Italian context across different urban realities and, despite the high specificity of the territory, our findings experimentally confirm what was stated in previous studies (Mascarenhas et al., 2019; Sebastiani et al., 2021), in which the dense urban fabric was considered irreconcilable with a positive ESs supply–demand balance.

Declaration of Competing Interest

The authors declare that they have no known competing financial interests or personal relationships that could have appeared to influence the work reported in this paper.

Data availability

Data will be made available on request.

Acknowledgments

Research grants: 2021 @CNR project BIOCITY "Riforestazione

urbana: nuovi strumenti conoscitivi e di supporto decisionale"; PRIN2020-MULTIFOR "Multi-scale observations to predict Forest response to pollution and climate change" funded by the Ministry of Research; CIR01_00019—PRO-ICOS_MED Potenziamento della Rete di Osservazione ICOS-Italia nel Mediterraneo—Rafforzamento del capitale umano" funded by the Ministry of Research; project n. 36388 TECNO-VERDE: "Tecnologie geomatiche e ambientali di precisione per il monitoraggio e la valorizzazione dei servizi ecosistemici delle infrastrutture verdi urbane e peri-urbane" funded by Regione Lazio; Project "National Biodiversity Future Center—NBFC" (code CN_00000033), funded by the Italian Ministry of University and Research; Next Generation EU Mission 4 "Education and Research" – Component 2: "From research to business" – Investment 3.1: "Fund for the realisation of an integrated system of research and innovation infrastructures" – Project IR0000032 – ITINERIS – Italian Integrated Environmental Research Infrastructures System – CUP B53C22002150006.We thank the Regional Agencies for Environmental Protection (ARPA) of Lombardia, Emilia Romagna, Lazio and Puglia for air quality data provisioning.

Appendix A. Supplementary data

Supplementary data to this article can be found online at https://doi.org/10.1016/j.ecolind.2023.110928.

References

Anderson, J.R., Hardy, E.E., Roach, J.T., Witmer, R.E., 1976. A land use land cover classification system for use with remote sensor data. US Government Printing Office, Washington, D. C.

Angelini P., Augello R., Bianco P.M., Gennaio R., La Ghezza V., Lavarra P., Marrese M., Papallo O., Perrino V. M., Sani R., M. Stelluti. 2012. Carta della Natura della Regione Puglia: Carta degli habitat alla scala 1:50.000. ISPRA.

Armondi, S., Di Vita, S., 2017. Milan: productions, spatial patterns and urban change. Routledge.

Balzan, M.V., Zulian, G., Maes, J., Borg, M., 2021. Assessing urban ecosystem services to prioritise nature-based solutions in a high-density urban area. Nature-Based Solutions 1, 100007. https://doi.org/10.1016/j.nbsj.2021.100007.

Baró, F., Haase, D., Gómez-Baggethun, E., Frantzeskaki, N., 2015. Mismatches between ecosystem services supply and demand in urban areas: A quantitative assessment in five European cities. Ecological Indicators 55, 146–158. https://doi.org/10.1016/j.ecolind.2015.03.013.

Baró, F., Palomo, I., Zulian, G., Vizcaino, P., Haase, D., Gómez-Baggethun, E., 2016. Mapping ecosystem service capacity, flow and demand for landscape and urban planning: A case study in the Barcelona metropolitan region. Land Use Policy 57, 405–417. https://doi.org/10.1016/j.landusepol.2016.06.006.

Blasi, C., Capotorti, G., Alós Ortí, M.M., Anzellotti, I., Attorre, F., Azzella, M.M., Carli, E., Copiz, R., Garfì, V., Manes, F., Marando, F., Marchetti, M., Mollo, B., Zavattero, L., 2017. Ecosystem mapping for the implementation of the European Biodiversity Strategy at the national level: The case of Italy. Environmental Science & Policy 78, 173–184. https://doi.org/10.1016/j.envsci.2017.09.002.

Bussotti, F., 2008. Functional leaf traits, plant communities and acclimation processes in relation to oxidative stress in trees: a critical overview. Global Change Biology 14, 2727–2739. https://doi.org/10.1111/j.1365-2486.2008.01677.x.

Cardillo A., Ceralli D., Canali E., Laureti L., D'Angeli C., Augello R., 2021. Carta della Natura della Regione Emilia-Romagna: carta degli habitat alla scala 1:25.000. ISPRA.

Casella L., Agrillo E., Cardillo A., Carbone M., Cattena C., Laureti L., Lugari A., Spada F., 2008. Carta della Natura della Regione Lazio: Carta degli habitat alla scala 1:50.000. ISPRA.

Chen, J., Jiang, B., Bai, Y., Xu, X., Alatalo, J.M., 2019. Quantifying ecosystem services supply and demand shortfalls and mismatches for management optimisation. Science of The Total Environment 650, 1426–1439. https://doi.org/10.1016/j.scitotenv.2018.09.126.

Chen, J., Tang, J., Yu, X., 2020. Environmental and physiological controls on diurnal and seasonal patterns of biogenic volatile organic compound emissions from five dominant woody species under field conditions. Environmental Pollution 259, 113955. https://doi.org/10.1016/j.envpol.2020.113955.

CMCC, 2022. Roma e il CLIMA: passato e futuro. Accessed at https://www.cmcc.it/it/report-roma in May 2023.

Cochran, W.G., 1977. Sampling Techniques, 3rd ed. John Wiley & Sons, New York.

Cohen-Shacham, E., Walters, G., Janzen, C., Maginnis, S., 2016. Nature-based solutions to address global societal challenges. IUCN: Gland. Switzerland 97, 2016–2036.

Combes, A., Franchineau, G., 2019. Fine particle environmental pollution and cardiovascular diseases. Metabolism, Role of Environment in Initiation and Progression of Illnesses 100, 153944. https://doi.org/10.1016/j.metabol.2019.07.008.

Congedo, L., 2021. Semi-Automatic Classification Plugin: A Python tool for the download and processing of remote sensing images in QGIS. Journal of Open Source Software, 6(64), 3172, 10.21105/joss.03172.

Cumming, G.S., Olsson, P., Chapin, F.S., Holling, C.S., 2013. Resilience, experimentation, and scale mismatches in social-ecological landscapes. Landscape Ecology 28 (6), 1139–1150.

dell'Agnese, E., Anzoise, V., 2011. Milan, the unthinking metropolis. International Planning Studies 16 (3), 217–235.

Diémoz, H., Gobbi, G.P., Magri, T., Pession, G., Pittavino, S., Tombolato, I.K.F., Campanelli, M., Barnaba, F., 2019. Transport of Po Valley aerosol pollution to the northwestern Alps – Part 2: Long-term impact on air quality. Atmospheric Chemistry and Physics 19, 10129–10160. https://doi.org/10.5194/acp-19-10129-2019.

Dupras, J., Alam, M., 2015. Urban Sprawl and Ecosystem Services: A Half Century Perspective in the Montreal Area (Quebec, Canada). Journal of Environmental Policy & Planning 17, 180–200. https://doi.org/10.1080/1523908X.2014.927755.

European Commission, 2020. EU Biodiversity Strategy for 2030. Retrieved on September 2022 from. https://eur-lex.europa.eu/resource.html?uri=cellar:a3c806a6-9ab3-11ea-9d2d-01aa75ed71a1.0001.02/DOC_1&format=PDF.

European Commission, 2021. Pathway to a Healthy Planet for All. EU Action Plan: 'Towards Zero Pollution for Air, Water and Soil'. Accessed at https://eur-lex.europa.eu/legal-content/EN/TXT/HTML/?uri=CELEX:52021DC0400&from=EN in May 2023.

European Environment Agency, 2018a. Air Quality in Europe - 2018 Report. EEA Report No 12/2018. ISSN: 1977-8449. doi: 10.2800/777411.

European Environment Agency, 2018b. Corine Land Cover 2018; Version 2020_20u1; European Environment Agency: Copenhagen, Denmark, 2020. Accessed at: https://land.copernicus.eu/pan-european/corine-land-cover/clc2018 in October 2022.

European Environment Agency, 2018c. Urban Atlas, Copernicus Land Monitoring Service. Accessed at https://land.copernicus.eu/local/urban-atlas in May 2023. European Environment Agency, 2022. Air Quality in Europe – 2022 Report. Accessed at https://www.eea.europa.eu/publications/air-quality-in-europe-2022 in May 2023 + Italy Air pollution factsheet. Accessed at https://www.eea.europa.eu/themes/air/country-fact-sheets/2022-country-fact-sheets/italy-air-pollution-country in May 2023.

European Space Agency (ESA), 2015. Sentinel-2 User Handbook. Accessed at https://sentinel.esa.int/documents/247904/685211/Sentinel2_User_Handbook.pdf/8869acdf-fd84-43ec-ae8c-3e80a436a16c?t=1438278087000 in January 2023Fares, S., Conte, A., Alivernini, A., Chianucci, F., Grotti, M., Zappitelli, I., Petrella, F., Corona, P., 2020. Testing Removal of Carbon Dioxide, Ozone, and Atmospheric Particles by Urban Parks in Italy. Environmental Science & Technology 54, 14910–14922. https://doi.org/10.1021/acs.est.0c04740.

Filippini, T., Rothman, K.J., Cocchio, S., Narne, E., Mantoan, D., Saia, M., Goffi, A., Ferrari, F., Maffeis, G., Orsini, N., Baldo, V., Vinceti, M., 2021. Associations between mortality from COVID-19 in two Italian regions and outdoor air pollution as assessed through tropospheric nitrogen dioxide. Science of The Total Environment 760, 143355. https://doi.org/10.1016/j.scitotenv.2020.143355.

Fitzky, A.C., Sandén, H., Karl, T., Fares, S., Calfapietra, C., Grote, R., Saunier, A., Rewald, B., 2019. The Interplay Between Ozone and Urban Vegetation—BVOC Emissions, Ozone Deposition, and Tree Ecophysiology. Frontiers in Forests and Global. Change 2.

Fusaro, L., Salvatori, E., Winkler, A., Frezzini, M.A., De Santis, E., Sagnotti, L., Canepari, S., Manes, F., 2021. Urban trees for biomonitoring atmospheric particulate matter: An integrated approach combining plant functional traits, magnetic and chemical properties. Ecological Indicators 126, 107707. https://doi.org/10.1016/j.ecolind.2021.107707.

Gerosa, G., Marzuoli, R., Desotgiu, R., Bussotti, F., Ballarin-Denti, A., 2009. Validation of the stomatal flux approach for the assessment of ozone visible injury in young forest trees. Results from the TOP (transboundary ozone pollution) experiment at Curno, Italy. Environmental Pollution, Special Issue Section: Ozone and Mediterranean Ecology: Plants, People, Problems 157, 1497–1505. https://doi.org/10.1016/j.envpol.2008.09.042.

González-García, A., Palomo, I., González, J.A., López, C.A., Montes, C., 2020. Quantifying spatial supply-demand mismatches in ecosystem services provides insights for land-use planning. Land Use Policy 94, 104493. https://doi.org/10.1016/j.landusepol.2020.104493.

Grimm, N.B., Faeth, S.H., Golubiewski, N.E., Redman, C.L., Wu, J., Bai, X., Briggs, J.M., 2008. Global Change and the Ecology of Cities. Science 319, 756–760. https://doi.org/10.1126/science.1150195.

IPCC, 2023. AR6 Synthesis Report: Climate Change 2023. Accessed at https://www.ipcc.ch/report/sixth-assessment-report-cycle/in May 2023.

ISPRA, 2021. Carta nazionale del consumo di suolo 2019 (risoluzione 10 m) v.1.0 26/07/2021. Accessed at https://groupware.sinanet.isprambiente.it/uso-copertura-e-consumo-di-suolo/library/consumo-di-suolo/carta-nazionale-consumo-suolo-2019 in October 2022.

ISPRA, 2022. Consumo di suolo, dinamiche territoriali e servizi ecosistemici. Edizione 2022. Report SNPA n. 32/2022 – ISBN 978-88-448-1124-2 P. 76.

ISTAT, 2020. Annuario Statistico italiano 2020. Accessed at https://www.istat.it/it/archivio/251048 in May 2023.

ISTAT, 2022. Annuario Statistico italiano 2022. Accessed at https://www.istat.it/storage/ASI/2022/ASI_2022.pdf in May 2023.

Jolliffe, I., 2005. Principal Component Analysis, in: Encyclopedia of Statistics in Behavioral Science. John Wiley & Sons, Ltd. 10.1002/0470013192.bsa501.

Karlsson, P.E., Klingberg, J., Engardt, M., Andersson, C., Langner, J., Karlsson, G.P., Pleijel, H., 2017. Past, present and future concentrations of ground-level ozone and potential impacts on ecosystems and human health in northern Europe. Science of

The Total Environment 576, 22–35. https://doi.org/10.1016/j.scitotenv.2016.10.061.
Krzyzanowski, M., Apte, J.S., Bonjour, S.P., Brauer, M., Cohen, A.J., Prüss-Ustun, A.M., 2014. Air Pollution in the Mega-cities. Curr Envir Health Rpt 1, 185–191. https://doi.org/10.1007/s40572-014-0019-7.
Legambiente, 2022. Mal'aria 2022 – edizione autunnale. Accessed at Verso città mobilità emissioni zero. https://www.legambiente.it/comunicati-stampa/malaria-2022-edizione-autunnale-verso-citta-mobilita-emissioni-zero/in May 2023.
Manes, F., Incerti, G., Salvatori, E., Vitale, M., Ricotta, C., Costanza, R., 2012. Urban ecosystem services: tree diversity and stability of tropospheric ozone removal. Ecological Applications 22, 349–360. https://doi.org/10.1890/11-0561.1.
Manes, F., Silli, V., Salvatori, E., Incerti, G., Galante, G., Fusaro, L., Perrino, C., 2014. URBAN ECOSYSTEM SERVICES: TREE DIVERSITY AND STABILITY OF PM10 REMOVAL IN THE METROPOLITAN AREA OF ROME. Annali di Botanica 4, 19–26. https://doi.org/10.4462/annbotrm-11746.
Manes, F., Marando, F., Capotorti, G., Blasi, C., Salvatori, E., Fusaro, L., Ciancarella, L., Mircea, M., Marchetti, M., Chirici, G., Munafò, M., 2016. Regulating Ecosystem Services of forests in ten Italian Metropolitan Cities: Air quality improvement by PM10 and O3 removal. Ecological Indicators 67, 425–440. https://doi.org/10.1016/j.ecolind.2016.03.009.
Marando, F., Salvatori, E., Sebastiani, A., Fusaro, L., Manes, F., 2019. Regulating Ecosystem Services and Green Infrastructure: assessment of Urban Heat Island effect mitigation in the municipality of Rome, Italy. Ecological Modelling 392, 92–102. https://doi.org/10.1016/j.ecolmodel.2018.11.011.
Mascarenhas, A., Haase, D., Ramos, T.B., Santos, R., 2019. Pathways of demographic and urban development and their effects on land take and ecosystem services: The case of Lisbon Metropolitan Area, Portugal. Land Use Policy 82, 181–194. https://doi.org/10.1016/j.landusepol.2018.11.056.
McDonald, R.I., Mansur, A.V., Ascensão, F., Colbert, M., Crossman, K., Elmqvist, T., Gonzalez, A., Güneralp, B., Haase, D., Hamann, M., Hillel, O., Huang, K., Kahnt, B., Maddox, D., Pacheco, A., Pereira, H.M., Seto, K.C., Simkin, R., Walsh, B., Werner, A. S., Ziter, C., 2020. Research gaps in knowledge of the impact of urban growth on biodiversity. Nat Sustain 3, 16–24. https://doi.org/10.1038/s41893-019-0436-6.
McPhearson, T., Cook, E.M., Berbes-Blazquez, M., Cheng, C., Grimm, N.B., Andersson, E., Barbosa, O., Chandler, D.G., Chang, H., Chester, M.V., 2022. A social-ecological-technological systems framework for urban ecosystem services. One Earth 5, 505–518.
Morillas, J.M.B., Gozalo, G.R., González, D.M., Moraga, P.A., Vílchez-Gómez, R., 2018. Noise Pollution and Urban Planning. Curr Pollution Rep 4, 208–219. https://doi.org/10.1007/s40726-018-0095-7.
Mudway, I.S., Dundas, I., Wood, H.E., Marlin, N., Jamaludin, J.B., Bremner, S.A., Cross, L., Grieve, A., Nanzer, A., Barratt, B.M., Beevers, S., Dajnak, D., Fuller, G.W., Font, A., Colligan, G., Sheikh, A., Walton, R., Grigg, J., Kelly, F.J., Lee, T.H., Griffiths, C.J., 2019. Impact of London's low emission zone on air quality and children's respiratory health: a sequential annual cross-sectional study. The Lancet Public Health 4, e28–e40. https://doi.org/10.1016/S2468-2667(18)30202-0.
Mullin, K., Mitchell, G., Nawaz, N.R., Waters, R.D., 2018. Natural capital and the poor in England: Towards an environmental justice analysis of ecosystem services in a high income country. Landscape and Urban Planning 176, 10–21. https://doi.org/10.1016/j.landurbplan.2018.03.022.
Nardella, L., Sebastiani, A., Stafoggia, M., Franzese, P.P., Manes, F., 2023. Modelling PM10 removal in three Italian coastal Metropolitan Cities along a latitudinal gradient. Ecological Modelling 483, 110423. https://doi.org/10.1016/j.ecolmodel.2023.110423.
Nowak, D.J., 1994. Air pollution removal by Chicago's urban forest. Chicago's urban forest ecosystem: Results of the Chicago urban forest climate project 63–81.
Oloffson, P., Foody, G.M., Herold, M., Stehman, S.V., Woodcock, C.E., Wulder, M.A., 2014. Good practices for estimating area and assessing accuracy of land change. Remote Sensing of Environment 148, 42–57. https://doi.org/10.1016/j.rse.2014.02.015.
Orioli, R., Antonucci, C., Scortichini, M., Cerza, F., Marando, F., Ancona, C., Manes, F., Davoli, M., Michelozzi, P., Forastiere, F., Cesaroni, G., n.d. Exposure to Residential Greenness as a Predictor of Cause-Specific Mortality and Stroke Incidence in the Rome Longitudinal Study. Environmental Health Perspectives 127, 027002. 10.1289/EHP2854.
Raymond, C.M., Frantzeskaki, N., Kabisch, N., Berry, P., Breil, M., Nita, M.R., Geneletti, D., Calfapietra, C., 2017. A framework for assessing and implementing the co-benefits of nature-based solutions in urban areas. Environmental Science & Policy 77, 15–24. https://doi.org/10.1016/j.envsci.2017.07.008.
Ringnér, M., 2008. What is principal component analysis? Nature Biotechnology 26, 303–304. https://doi.org/10.1038/nbt0308-303.
Salvati, L., Carlucci, M., 2015. Land-use structure, urban growth, and periurban landscape: A multivariate classification of the European cities. Environment and Planning B: Planning and Design 42, 801–829.
Salvati, L., Carlucci, M., 2016. Patterns of Sprawl: The Socioeconomic and Territorial Profile of Dispersed Urban Areas in Italy. Regional Studies 50, 1346–1359. https://doi.org/10.1080/00343404.2015.1009435.
Salvati, L., Zambon, I., Chelli, F.M., Serra, P., 2018. Do spatial patterns of urbanization and land consumption reflect different socioeconomic contexts in Europe? Science of The Total Environment 625, 722–730. https://doi.org/10.1016/j.scitotenv.2017.12.341.
Salvatori, E., Fusaro, L., Manes, F., 2016. CHLOROPHYLL FLUORESCENCE FOR PHENOTYPING DROUGHT-STRESSED TREES IN A MIXED DECIDUOUS FOREST. Annali di Botanica 6, 39–49. https://doi.org/10.4462/annbotrm-13263.
Sanesi, G., Chiarello, F., 2006. Residents and urban green spaces: The case of Bari. Urban Forestry & Urban Greening 4, 125–134. https://doi.org/10.1016/j.ufug.2005.12.001.
Sarrat, C., Lemonsu, A., Masson, V., Guedalia, D., 2006. Impact of urban heat island on regional atmospheric pollution. Atmospheric Environment 40, 1743–1758. https://doi.org/10.1016/j.atmosenv.2005.11.037.
Schmalz, B., Kruse, M., Kiesel, J., Müller, F., Fohrer, N., 2016. Water-related ecosystem services in Western Siberian lowland basins—Analysing and mapping spatial and seasonal effects on regulating services based on ecohydrological modelling results. Ecological Indicators 71, 55–65. https://doi.org/10.1016/j.ecolind.2016.06.050.
Sebastiani, A., Marando, F., Manes, F., 2021. Mismatch of regulating ecosystem services for sustainable urban planning: PM10 removal and urban heat island effect mitigation in the municipality of Rome (Italy). Urban Forestry & Urban Greening 57, 126938. https://doi.org/10.1016/j.ufug.2020.126938.
Semeraro, T., Scarano, A., Buccolieri, R., Santino, A., Aarrevaara, E., 2021. Planning of Urban Green Spaces: An Ecological Perspective on Human Benefits. Land 10, 105. https://doi.org/10.3390/land10020105.
Shi, Y., Shi, D., Zhou, L., Fang, R., 2020. Identification of ecosystem services supply and demand areas and simulation of ecosystem service flows in Shanghai. Ecological Indicators 115, 106418. https://doi.org/10.1016/j.ecolind.2020.106418.
Sicard, P., Agathokleous, E., Araminiene, V., Carrari, E., Hoshika, Y., De Marco, A., Paoletti, E., 2018. Should we see urban trees as effective solutions to reduce increasing ozone levels in cities? Environmental Pollution 243, 163–176. https://doi.org/10.1016/j.envpol.2018.08.049.
Tétreault, L.-F., Doucet, M., Gamache, P., Fournier, M., Brand, A., Kosatsky, T., Smargiassi, A., 2016. Severe and Moderate Asthma Exacerbations in Asthmatic Children and Exposure to Ambient Air Pollutants. International Journal of Environmental Research and Public Health 13, 771. https://doi.org/10.3390/ijerph13080771.
The Organisation for Economic Co-Operation and Development (OECD), 2008. Annual Report 2008. Accessed at https://www.oecd.org/newsroom/40556222.pdf in May 2023.
Tomson, M., Kumar, P., Barwise, Y., Perez, P., Forehead, H., French, K., Morawska, L., Watts, J.F., 2021. Green infrastructure for air quality improvement in street canyons. Environment International 146, 106288. https://doi.org/10.1016/j.envint.2020.106288.
Traversi, D., Degan, R., De Marco, R., Gilli, G., Pignata, C., Villani, S., Bono, R., 2009. Mutagenic properties of PM2.5 urban pollution in the Northern Italy: The nitro-compounds contribution. Environment International 35, 905–910. https://doi.org/10.1016/j.envint.2009.03.010.
United Nations, 2015. Accesed at https://sdgs.un.org/2030agenda in May 2023.
Vignoli, F., de Luca, C., Tondelli, S., 2021. A spatial ecosystem services assessment to support decision and policy making: The case of the city of Bologna. Sustainability 13 (5), 2787.
Villamagna, A.M., Angermeier, P.L., Bennett, E.M., 2013. Capacity, pressure, demand, and flow: A conceptual framework for analyzing ecosystem service provision and delivery. Ecological Complexity 15, 114–121. https://doi.org/10.1016/j.ecocom.2013.07.004.
Winkler, K.J., Dade, M.C., Rieb, J.T., 2021. Mismatches in the Ecosystem Services Literature—a Review of Spatial, Temporal, and Functional-Conceptual Mismatches. Curr Landscape Ecol Rep 6, 23–34. https://doi.org/10.1007/s40823-021-00063-2.
Wood, S.L.R., Dupras, J., 2021. Increasing functional diversity of the urban canopy for climate resilience: Potential tradeoffs with ecosystem services? Urban Forestry & Urban Greening 58, 126972. https://doi.org/10.1016/j.ufug.2020.126972.
Overview [WWW Document], World Bank, 2022. URL https://www.worldbank.org/en/topic/urbandevelopment/overview (accessed 5.23.23).
Wu, D., Lin, J.C., Oda, T., Kort, E.A., 2020. Space-based quantification of per capita CO2 emissions from cities. Environmental Research Letters 15, 035004. https://doi.org/10.1088/1748-9326/ab68eb.
Yao, J., Liu, M., Chen, N., Wang, X., He, X., Hu, Y., Wang, X., Chen, W., 2021. Quantitative assessment of demand and supply of urban ecosystem services in different seasons: a case study on air purification in a temperate city. Landscape Ecology 36, 1971–1986. https://doi.org/10.1007/s10980-020-01112-7.
Yuan, Y., Chen, D., Wu, S., Mo, L., Tong, G., Yan, D., 2019. Urban sprawl decreases the value of ecosystem services and intensifies the supply scarcity of ecosystem services in China. Science of The Total Environment 697, 134170. https://doi.org/10.1016/j.scitotenv.2019.134170.
Zambon, I., Salvati, L., 2019. Metropolitan growth, urban cycles and housing in a Mediterranean country, 1910s–2010s. Cities 95, 102412. https://doi.org/10.1016/j.cities.2019.102412.
Zappitelli, I., Conte, A., Alivernini, A., Finardi, S., Fares, S., 2023. Species-Specific Contribution to Atmospheric Carbon and Pollutant Removal: Case Studies in Two Italian Municipalities. Atmosphere 14, 285. https://doi.org/10.3390/atmos14020285.